Supplementary Material

Portable fluorescent conjugated microporous polymer sensor coupled with a smartphone for on-site Fe^{3+} detection in water

Lei Chen[a,‡], Xiaomin Mai[a,‡], Wannan Lai[a], Guangyu Ge[a], Ran Ma[a], Yongning Wu[b] , Qinghua He[a,c*]

[a] Department of Food Science and Engineering, College of Chemistry and Environmental Engineering, Shenzhen University, Shenzhen 518060, China;

[b] Food Safety Research Unit (2019RU014) of Chinese Academy of Medical Science, NHC Key Laboratory of Food Safety Risk Assessment, China National Center for Food Safety Risk Assessment, Beijing 100021, China;

[c] Shenzhen Key Laboratory of Food Macromolecules Science and Processing, Shenzhen University, Shenzhen 518060, China;

‡ Lei Chen and Xiaomin Mai contributed equally to this manuscript;

* Corresponding author: Qinghua He, E-mail address: qinghua.he@szu.edu.cn

Table of Contents

1. Characterization methods and instruments

The morphology of THDH-DMA was characterized using scanning electron microscopy (SEM) (JSM-7800F & TEAM Octane Plus, JEOL Co., Japan). The internal structure of THDH-DMA was characterized using Transmission electron microscopy (TEM) (JEM-2100 & X-Max80, JEOL Co., Japan). The powder X-ray diffraction (PXRD) spectra were recorded on an Empyrean diffractometer (PANalytical, Netherlands) with Cu-Kα radiation (λ = 0.15406 nm), employing a scanning rate of 10°/min and a step size of 0.01°. The characteristic functional groups of the materials were obtained using Fourier transform infrared spectroscopy (FT-IR) (IR Affinity-1, Shimadzu, Japan) across the range of 400-4000 cm^{-1}. Brunauer-Emmett-Teller (BET) specific surface area and pore size distribution of THDH-DMA were determined by Nitrogen adsorption/desorption isotherm measurements under a liquid nitrogen atmosphere of 77 K (BELSORP-MAX, MicrotracBEL Corp, Japan). Thermostability was measured by thermogravimetric analysis (TGA) instrument (STA449 F5, NETZSCH-Gerätebau GmbH, Germany) by heating samples from 25 °C to 800 °C under a nitrogen atmosphere. X-ray photoelectron spectroscopy (XPS) was recorded on a Thermo Scientific K-Alpha instrument (K-Alpha, Thermo Fisher Scientific, UK). All fluorescence spectra were measured via a fluorescence spectrometer (F-7000, Hitachi, Japan). The excitation and emission slits were set to a width of 2.5 nm, and the voltage was maintained at 700 V.

2. Materials and methods

2.1. Chemicals and materials

Hydrochloric acid (HCl) and sodium hydroxide (NaOH) were sourced from Shanghai Aladdin Biochemical Technology Co., Ltd. (Shanghai, China). All other reagents and

materials were supplied by Shanghai Macklin Biochemical Technology Co., Ltd. (Shanghai, China). All chemicals and reagents were of analytical reagent grade or higher purity and were utilized as received without additional purification. Ultrapure water was obtained from a Milli-Q Advantage water purification system (Merck KGaA, Darmstadt, Germany).

2.2. Synthesis of THDH-DMA

THDH (29.12 mg, 0.15 mmol) and DMA (29.12 mg, 0.15 mmol) were dissolved in a solvent mixture of o-dichlorobenzene (1.7 mL) and n-butanol (0.3 mL) under ultrasonication for 10 min. After the addition of 6 M acetic acid (0.1 mL), sonication was continued for another 5 min. The homogeneous mixture was transferred to a 10 mL Schlenk tube, subjected to three freeze-pump-thaw degassing cycles, and thermally reacted at 120°C for 72 h. After completion of the reaction, the crude product was purified by sequential washing with THF and DMF (repeated cycles) to remove unreacted precursors and byproducts. Finally, the purified solid was vacuum-dried at 100°C for 12 h to afford a bright yellow powder.

2.3. Fluorescence detection method

THDH-DMA (1 mg) was dissolved in DMF (10 mL) and sonicated for 10 min to form a homogeneous suspension. Stock solutions of Fe^{3+}, K^{+}, Na^{+}, As^{3+}, Mn^{2+}, Hg^{2+}, Co^{2+}, Ag^{+}, Cu^{2+}, Zn^{2+}, and Ni^{2+} were diluted in ultrapure water to prepare metal ion working solutions. Fluorescence spectroscopy was employed to determine the optimal excitation and emission wavelengths, optimize the optimal solvent and detection pH, and evaluate the detection response time of THDH-DMA toward Fe^{3+}.

Fluorescence intensities of THDH-DMA suspensions spiked with Fe^{3+} at varying concentrations (0.01, 0.05, 0.10, 0.50, 1.00, 2.00, 3.00, 4.00, 5.00, 6.00, 7.00, 8.00, 9.00, and

10.00 mg/L) were recorded using an F-7000 fluorescence spectrophotometer. The linear detection range was calculated using the Stern-Volmer equation: $I_0/I = 1+Ksv[M]$, where I_0 and I represent the fluorescence intensities of THDH-DMA before and after Fe^{3+} addition, respectively; [M] denotes the Fe^{3+} concentration (mg/L); and K_{sv} is a constant of the Stern-Volmer equation. The limit of detection (LOD) was determined by the equation $LOD = 3\sigma/k$, with σ defined as the standard deviation of the blank signal and *k* as the slope of the calibration curve.

The selectivity of THDH-DMA toward Fe^{3+} was evaluated by comparing the fluorescence quenching extent of suspensions after adding Fe^{3+} and other metal ions (10 mg/L). The degree of fluorescence quenching was expressed as I/I_0, where $I/I_0 = 1$ indicates constant fluorescence intensity, $I/I_0 > 1$ indicates fluorescence enhancement, and $I/I_0 < 1$ indicates fluorescence quenching. In addition, an equal concentration of interfering ion solution was added to the Fe^{3+} assay, and the fluorescence intensity of THDH-DMA in the mixed system was measured to test the immunity to interference for Fe^{3+} detection. Fluorescence measurements were performed at an excitation wavelength of 350 nm, with the emission spectra recorded in the 370-680 nm range under identical experimental conditions. To ensure reproducibility, all experiments were conducted in triplicate.

2.4. Detection of Fe^{3+} in real water samples

Mineral water was purchased from Hangzhou Nongfu Spring Co., Ltd., whereas tap water was directly obtained from the laboratory water supply. Before analysis, all aqueous samples were filtered through sterile 0.22 μm syringe filters, followed by fortification with standard Fe^{3+} solutions to obtain final concentrations of 0.5, 2, and 5 mg/L. After adding

THDH-DMA to the solution, the fluorescence intensity was measured and used to calculate the recovery and relative standard deviation (RSD).

2.5. Constructing the smartphone-integrated sensing platform of Fe^{3+}

A smartphone-integrated sensing platform was developed for the intelligent visual detection of Fe^{3+}, utilizing the Color Picker Version 3.1 app (iOS 18.4.1) in conjunction with fluorescent THDH-DMA test strips. The test strips were immersed in a THDH-DMA suspension for 4 min, air-dried at room temperature, and subjected to three repeated cycles of drying and immersion to obtain THDH-DMA fluorescent test strips. The test strips were immersed in different concentrations of Fe^{3+} (0-10 mg/L) solution for 1 minute. After drying, the strips were irradiated with a 365 nm UV light at an irradiation angle of 90° and a range of 20 cm in a dark chamber. Fluorescence images were captured at a fixed mobile phone focal distance to improve data accuracy and reproducibility. A linear regression model between Fe^{3+} concentration and the corresponding RGB values was established using the Color Picker Version 3.1 App, enabling quantitative determination of Fe^{3+} in the samples for intelligent detection.

3. Figures

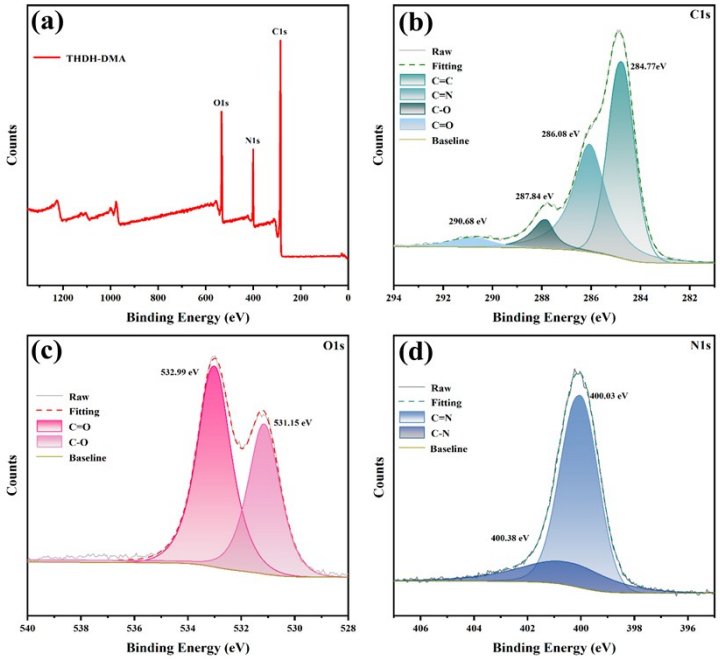

Figure S1. (a) The XPS spectrum of THDH-DMA. (b) XPS spectrum of the C 1s region of THDH-DMA. (c) XPS spectrum of the N 1s region of THDH-DMA. (d) XPS spectrum of the O 1s region of THDH-DMA.

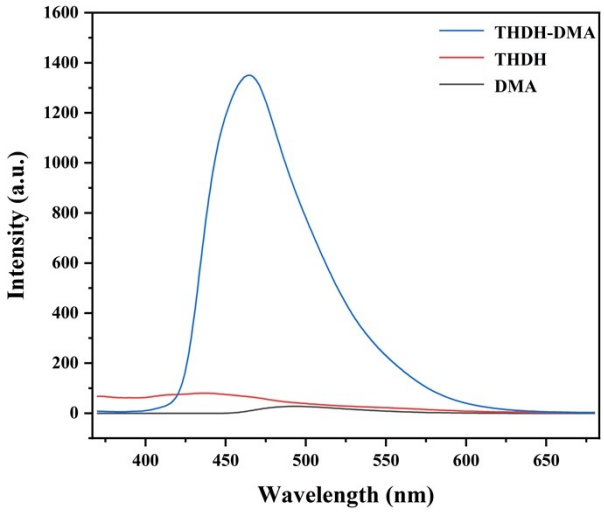

Figure S2. Fluorescence spectra of THDH-DMA, DMA, and THDH.

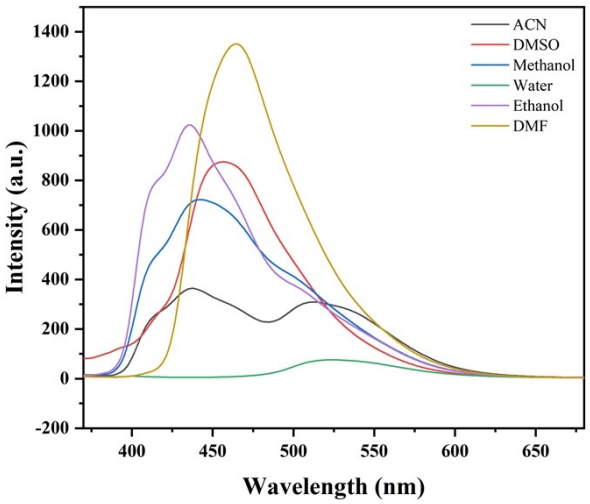

Figure S3. Changes in fluorescence intensity of THDH-DMA in different solvents.

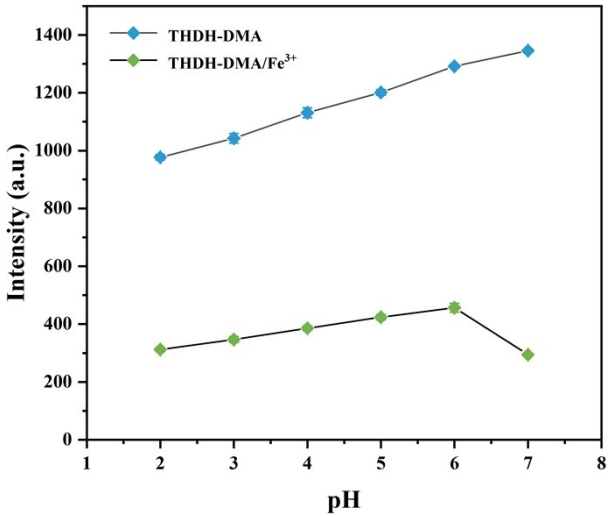

Figure S4. Changes in fluorescence intensity of THDH-DMA after the addition of Fe^{3+} at different pH values.

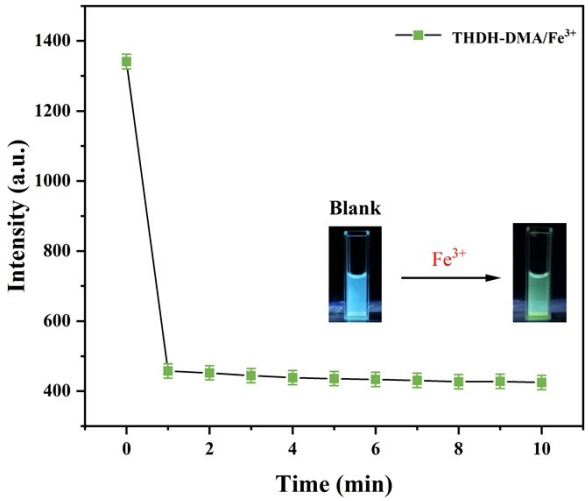

Figure S5. Changes in fluorescence intensity of THDH-DMA with time after the addition of Fe^{3+}.

4. Tables

Table S1. Comparison of fluorescence sensors for Fe^{3+} detection.

Fluorescence sensors	Linear range (mg/L)	LOD (mg/L)	Matrix	Refs.
UHCOP	0.28-78.18	0.14	Tap water	1
NC-PDs	0-6.70	0.0715	Tap water	2
POP-HT	5-600	5	-	3
TTPE-COF	0.56-558.45	0.17	-	4
Ethylenediamine-CDs	0.45-4.47	0.21	Tap water	5
Green-CDs	1.68-33.51	0.53	Underground water, tap water	6
CCQDs	0-10.1	0.214	Lake water	7
THDH-DMA CMP	0.01-9	0.0038	Tap water, Mineral water	This work

Table S2. Performances of Fe^{3+} detection in real water samples using THDH-DMA (**n = 3**)

Samples	Added (mg/L)	Found ± SD (mg/L)	RSDs (%)	Recovery (%)
Tap water	0	ND*	-	-
	0.5	0.49 ± 0.14	2.88	97.99
	2	2.01 ± 0.22	1.08	100.73
	5	5.11 ± 1.36	2.67	102.17
Mineral water	0	ND	-	-
	0.5	0.52 ± 0.11	2.15	104.55
	2	1.98 ± 0.54	2.72	99.20
	5	5.16 ± 0.63	1.21	103.21

* ND: Not detectable

5. Reference

1. S. L. Ji, S. S. Xiao and L. L. Wang, *Spectrochim. Acta - A: Mol. Biomol. Spectrosc.*, 2022, **280**, 121541.
2. F. Vahedi, N. Arsalani and M. Amjadi, *J. Fluoresc.*, 2025, **35**, 9127-9135.
3. D. X. Ma, B. Y. Li, Z. H. Cui, K. Liu, C. L. Chen, G. H. Li, J. Hua, B. H. Ma, Z. Shi and S. H. Feng, *ACS Appl. Mater. Interfaces*, 2016, **8**, 24097-24103.
4. D. Cui, X. S. Ding, W. Xie, G. J. Xu, Z. M. Su, Y. H. Xu and Y. Z. Xie, *Crystengcomm*, 2021, **23**, 5569-5574.
5. Y. Q. Chen, X. B. Sun, W. Pan, G. F. Yu and J. P. Wang, *Front. Chem.*, 2020, **7**, 911.
6. M. Zulfajri, G. Gedda, C. J. Chang, Y. P. Chang and G. G. Huang, *ACS Omega*, 2019, **4**, 15382-15392.
7. K. X. Chen, Q. F. Chen and M. Zhu, *Int. J. Biol. Macromol.*, 2025, **309**, 142926.